J. Phys. Chem. A **2003,** *107,* 2954−2963

Gas-Phase Reaction Pathways from SiH_4 to Si_2H_6, Si_2H_4 and Si_2H_2: A Theoretical Study

Shao-Wen Hu,* Yi Wang, Xiang-Yun Wang, Ti-Wei Chu, and Xin-Qi Liu

Department of Applied Chemistry, College of Chemistry and Molecular Engineering, Peking University, Beijing, China 100871

Received: December 15, 2002; In Final Form: February 10, 2003

Initial gas-phase reactions for a system containing silane (SiH_4) and hydrogen (H_2) were investigated using ab initio calculations at the MP2/6-311++g** level. Twenty-four minimum and 19 transition states were located on the potential energy surface of the neutral species containing one or two silicon atoms. The bonding nature of each species was elucidated by topological analyses of electron density using Bader's AIM theory. The reaction pathways were classified into three parts: Part (I) shows elimination of the first H_2 and formation of disilane (Si_2H_6). Part (II) shows elimination of the second H_2 and formation of five disilene (Si_2H_4) isomers. Part (III) shows elimination of the third H_2 and formation of four disilyne (Si_2H_2) isomers. More energy is required to obtain species with less hydrogen content, and such species are more likely to be stabilized by a hydrogen bridged bond (Si−H−Si). Calculated IR spectra, dipole moments, and rotational constants were provided for comparison with the experiments.

I. Introduction

The simplest silicon hydride, SiH_4, is widely used as a building block in fabricating microelectronic silicon materials using chemical vapor deposition techniques. Before effective deposition to a solid surface, gas-phase reactions are usually induced.[1−6] Because of nucleation and fragmentation at various conditions, quite a number of species with different silicon−hydrogen proportions can form at this stage.[7−10] It is clear that the property of the solid product is closely related to the species generated in the gas phase.[11−14] The selective production of the species through controlling the gas phase or depositing conditions is, thus, very desirable. To this purpose, a good knowledge of the thermally activated chemistry of SiH_4 is of fundamental importance. Many experimental[15−18] and theoretical[18−25] investigations focus on the gas-phase reactions. Because the initial formation of the Si−Si bond and subsequent dissociation are supposed to be responsible for nucleation to larger Si_nH_{2n+2} clusters,[24,25] the detailed information concerning the prototype case involving one or two SiH_4 molecules deserves more attention. It has been proposed[17,24] that the rate-limiting step is SiH_4 decomposition into SiH_2 and H_2. SiH_2 then inserts readily into a Si−H bond of another SiH_4 to form Si_2H_6. Theoretically, two complexes consisted of SiH_2 and SiH_4 have been found to intermediate the insertion.[20,21] For this mechanism, there are questions remaining unanswered. In particular, experiments suggests that the insertion reaction is a three-body assisted association; otherwise, it is hard to explain the observed pressure dependence of the rate constants.[17] The structure of the loosely bonded complex from three body is still unclear. Besides nucleation to Si_2H_6, other relative transient species with one or two silicon atoms and less hydrogen content have been produced and detected experimentally. It was recently reported that several pathways starting from the decomposition of disilane have been revealed;[18] however, the pathways leading to some observed Si_2H_4 and Si_2H_2 isomers remains unclear. To model the gas-phase reactions in a more realistic way, it is necessary to elucidate mechanism pathways from SiH_4 to all possible species containing one or two silicon atoms. The purpose of this work is, therefore, to trace the detailed reaction pathways of such a system using ab initio calculations and topological analyses of electron densities. The theoretical investigation, involving all possible transient and stable intermediates and products, with the total system's energy varying within 120 kcal/mol, would provide useful information for understanding the mechanism and controlling the real gas-phase reactions.

TABLE 1: Comparison of the Calculated Enthalpy Changes ΔH (298°) with Experimental Values for Some Reactions

		ΔH (298°, kcal/mol)		
reactions[a,b]	symbol[b]	Mp2/6-31+G*[a]	G3//B3LY[b]	exptl[b]
$SiH_3SiH_3 =$				
SiH_4+SiH_2		54.3	52.1	54.3
$H_3SiSiH+H_2$		55.7	54.0	55.0
$H_2SiSiH_2+H_2$		47.6	46.7	46.6
SiH_3+SiH_2		70.3	75.3	76.7
SiH_3HSiH_2a _t (10)	TS1	50.5	43.7	53.4
SiH_3HSiH_2b_t (15)	TS2	50.2	43.1	
SiH_3SiH-H_2_t (33)	TS3	59.0	51.1	56.4
SiH_3SiH_t (26)	TS4	10.3	7.0	5.3
$H_2-SiH_2SiH_2$_t (21)	TS5	89.8	80.5	
SiH_3SiH_3 (eclipsed)		0.54	0.95	1.26

[a] Data based on calculations in this work. [b] Data from ref 18.

II. Calculation Method

All of the geometry structures were fully optimized at the MP2/6-31+G* level. Transition states were located using synchronous transit-guided quasi-Newtonian (STQN) methods[26] in combination with stepwise partial optimization along each pathway with one geometry parameter fixed as constant. Frequency calculations were performed following each optimi-

---

* To whom correspondence should be addressed. E-mail: sw-hu@163.com.

10.1021/jp027727p CCC: \$25.00

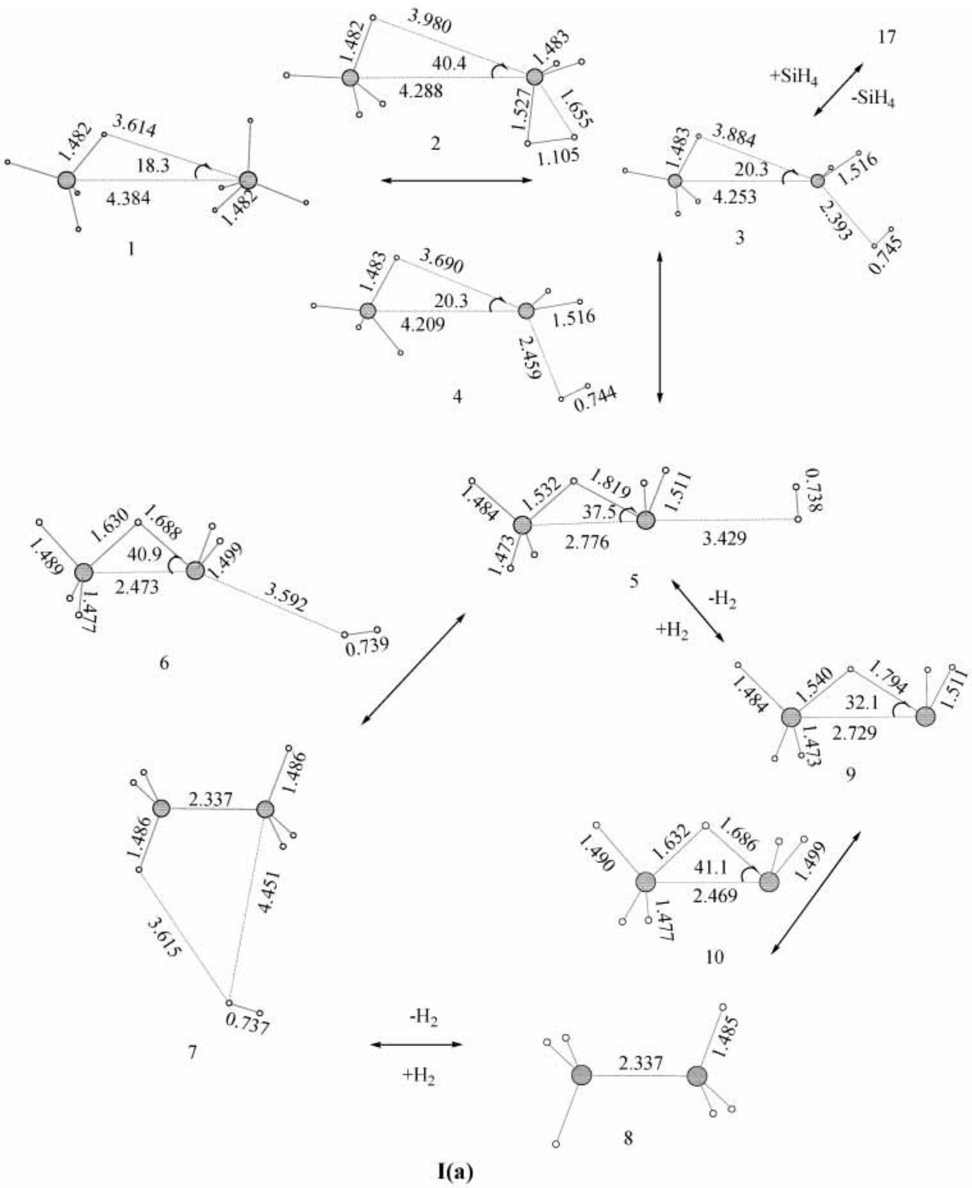

Figure 1. Optimized (MP2/6-31+G*) geometry structures of the species involved in the first H_2 elimination of the reaction paths (a). Bond lengths are in Å, angles are in degrees. The species on or under the double arrows are transition states.

zation to obtain the zero point energy (ZPE) and IR spectra data and to characterize all of the stationary points located on the potential energy surface. Single-point calculations at the MP2/6-311++g** level determine the electronic energies. The Guassian 98 program package[27] was employed for these calculations.

Wave functions calculated at the MP2/6-31+G* level were used for the topological analyses of the electron densities. The AIM2000 program[28] derived from Bader's "Atoms in Molecules" (AIM) theory[29] was employed for calculating the bond critical points (BCP) and bond paths and for drawing molecular graphs.

III. Results and Discussions

The MP2/6-31+G* calculated enthalpy changes for several process are compared with available data published by other people (Table 1). It can be seen that the results obtained by the MP2/6-31+G* calculation agree well with both experimental and the G3//B3LYP calculated results. Therefore, except for single-point energy calculations at the MP2/6-311++G**// MP2/6-31+G* level, higher level calculations were not performed.

In most cases, the dissociated H_2 is included as a weakly bonded fragment before it is separated completely. The structures of the weakly bonded complexes, obtained as we trace the mechanism pathways step by step, provide information concerning the direction of the dissociation or association. It may also help to understand the concentration and pressure dependence of the corresponding reactions.

The calculated reaction pathways (Figure 6, 7) are divided into three parts: Part I includes possible routes of first H_2 elimination and the formation of Si_2H_6. Part II includes possible routes of second H_2 elimination and formation of five Si_2H_4 isomers. Part III includes possible routes of third H_2 elimination and the formation of four Si_2H_2 isomers. The optimized geometry structures of all the transition states and minimums are classified into the three parts and arranged to show the reaction paths (Figures 1−4). Their numbering order, composition, electronic energy, dipole moment, and rotational constants

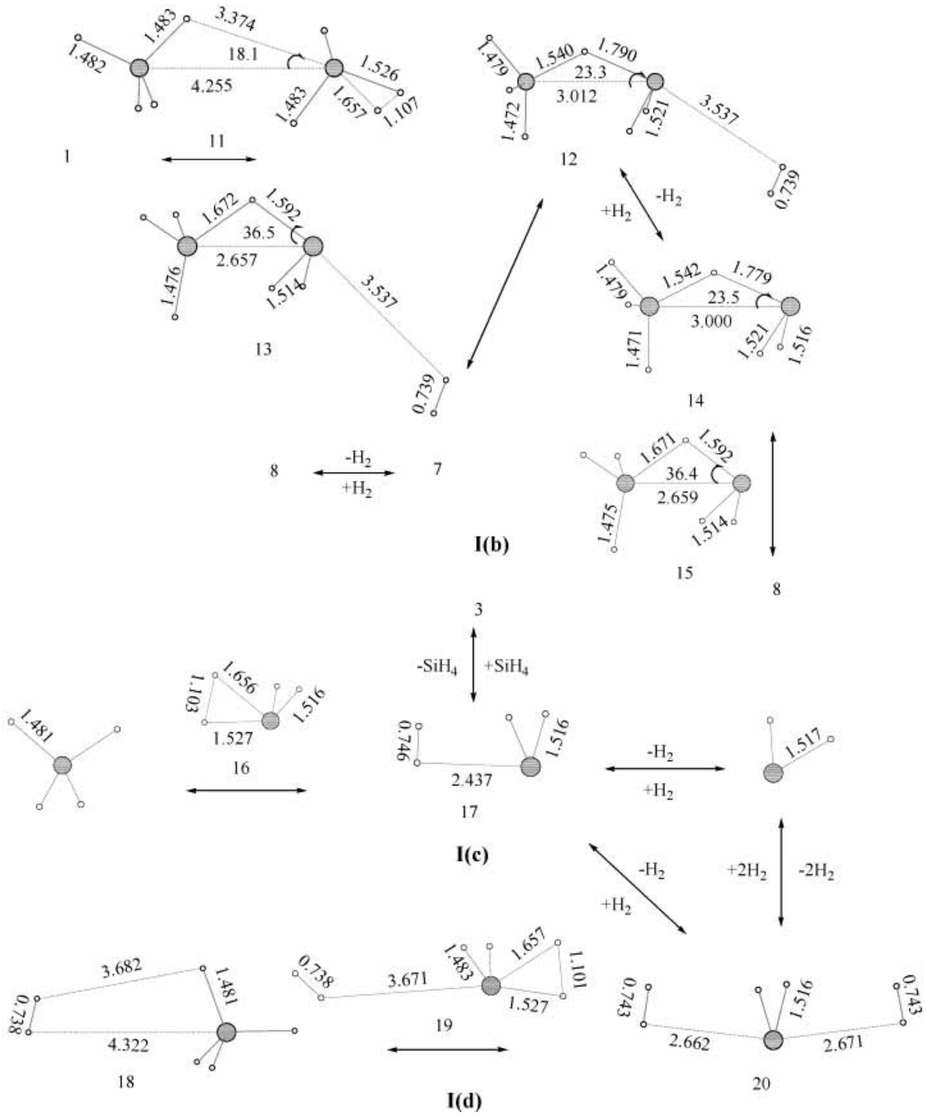

Figure 2. Optimized (MP2/6-31+G*) geometry structures of the species involved in the first H_2 elimination of the reaction paths (I(b)), (I(c)), and (I(d)). Bond lengths are in Å, angles are in degrees. The species on or under the double arrows are transition states.

are listed in Table 2. The molecular formula representing each species is written as close to its geometry structure as possible. Molecular graphs via AIM calculation are shown for all the stationary structures in Figure 5. The relative energies of the species evaluated as a system with total mass equal to that of SiH_4-SiH_4, SiH_4, or SiH_4-H_2 are listed in Table 3 and graphed in Figures 6 and 7. The IR spectra data for the minimum species are listed in Table 4.

Part (I): First H_2 Elimination and the Formation of Three Si_2H_6 Isomers. In the initial stage of a $SiH_4 + H_2$ mixture, three possible situations are considered. In the first case, the pressure of the total system and the density of SiH_4 are both high, and the molecular dimer SiH_4-SiH_4 (**1**) is likely to form. The two SiH_4 molecules are weakly dihydrogen-bonded to **1** according to the AIM calculation. The interaction energy is dispersive in nature and comparable with the methane dimer.[30] Two routes exist from **1** to the final disilane $SiH_3SiH_3-H_2$ (**7**). In route (a), **1** becomes the first intermediate minimum $SiH_4-SiH_2-H_2$ (**3**) over a barrier of transition state $SiH_4-SiH_2H_2a$_t (**2**). This is the rate-limiting step process as the system's energy increases to 60.62 kcal/mol relative to **1**. It can be seen that **3** is a loosely bonded complex consisting of three components, SiH_4, SiH_2, and H_2. However, the SiH_2 in **3** is obviously closer to H_2 than it to SiH_4. In other words, the first H_2 has not yet been completely eliminated from the SiH_2 group. Compound **3** then goes to a more stable intermediate complex, $SiH_3HSiH_2-H_2a$ (**5**), over a transition state $SiH_4-SiH_2-H_2$_t (**4**). From **3** to **5**, the fast process is a key step for full H_2 elimination and Si−Si bond formation. Through this step, the $Si-H_2$ distance becomes longer (from 2.393 to 3.429 Å), whereas the Si−Si bond becomes shorter (from 4.253 to 2.776 Å). The energy difference between (**3**) and (**5**) is 4.27 kcal/mol, which is the driving force for the process. Compound **5** is actually a hydrogen-bridged complex SiH_3HSiH_2a (**9**) weakly connected by a H_2. The process from **5** to **7** is essentially the same as from **9** to SiH_3SiH_3 (**8**). The total energy falls over a very small barrier transition state $SiH_3HSiH_2-H_2a$_t (**6**) or SiH_3HSiH_2a_t (**10**). Thus, the nucleation along route (a) is a three-step process. The first step is from **1** to H_2 partially eliminated **3**. The second step is from **3** to the H_2 fully eliminated and hydrogen-bridged intermediate complex **5**. The third step is the isomerization of **5** to disilane **7**. The nucleation can also proceed along route (b). The rate-limiting step is similar as in route (a) with a transition state $SiH_4-SiH_2H_2b$_t (**11**), an isomer of **2**, between **1** and $SiH_3HSiH_2-H_2b$ (**12**). Compound **12** is an isomer of **5** and is actually another hydrogen-bridged complex, SiH_3HSiH_2b (**14**), weakly connected to a H_2. Since **12** is the only intermediate minimum located between **1** and **7**, route (b) is a two-step

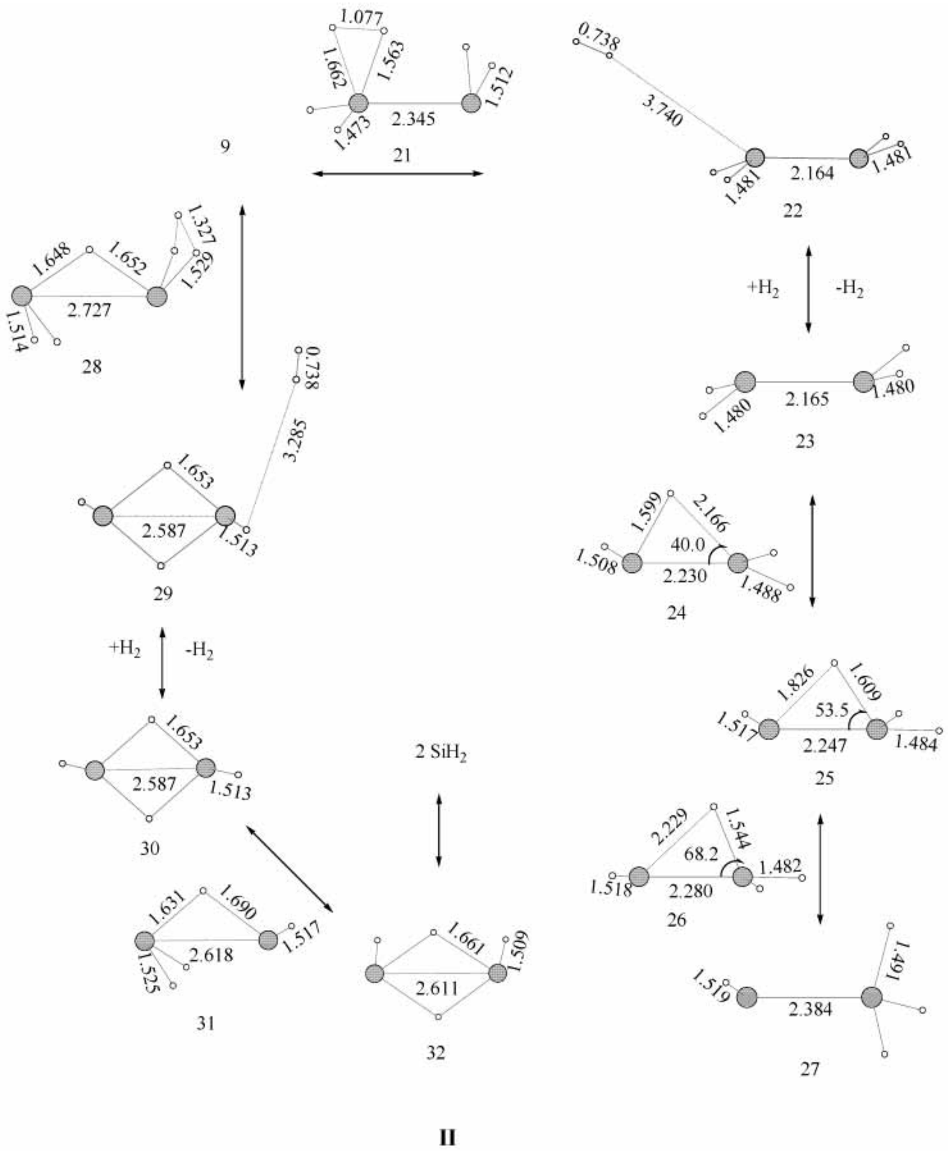

Figure 3. Optimized (MP2/6-31+G*) geometry structures of the species involved in the second H_2 elimination of the reaction paths (II). Bond lengths are in Å, angles are in degrees. The species on or under the double arrows are transition states.

process. The H_2 partially eliminated intermediate, like **3**, does not appear. The following isomerization from **12** through transition state $SiH_3HSiH_2{-}H_2b\_t$ (**13**) to **7**, again, is essentially the same as from **14** through transition state $SiH_3HSiH_2b\_t$ (**15**) to **8**. The two hydrogen-bridged intermediates **9** and **14** can be regarded as two Si_2H_6 isomers. Compared with the usual disilane **8**, it is obvious that the structures containing Si−H−Si bond are unstable, and isomerization can happen with very small barriers. It seems hard to separate routes (a) and (b) through temperature or pressure control. Considering the different dipole moments of the two intermediates **9** and **14**, the more polarized **14** may be likely to form in a polarized condition. In the second case, the pressure is assumed to be low, and SiH_4 is isolated as a single molecule. As shown in route (c), when energetically activated, SiH_4 undergoes self-dissociation into $SiH_2{-}H_2$ (**17**) over transition state $SiH_2{-}H_2\_t$ (**16**). Compound **17** is a complex of SiH_2 and H_2. It can be seen that the distance between the two fragments is quite short (2.437 Å), meaning the association is not negligibly weak. As a result, **17** may exist as a complex rather than dissociate into SiH_2 and H_2. The full dissociation, however, can happen as another body attacks in the direction opposite to the H_2 in **17**. If the attacker is another SiH_4, **5** or **12** will form, and the Si−Si bond will form. As we have indicated above, this can happen only when the pressure and density of SiH_4 are sufficiently high. If the attacker is another H_2, $H_2{-}SiH_2{-}H_2$ (**20**) will form. This is what happens in the third case along route (d). When the pressure and density of H_2 are assumed to be high, SiH_4 may be surrounded by H_2 or associated weakly into $SiH_4{-}H_2$ (**18**). The intermediate **20** will be back to **18** over a transition state $H_2{-}SiH_2{-}H_2\_t$ (**19**) whether going forward or backward. H_2 is clearly weak as an attacker. Nevertheless, the distance of H_2 to SiH_2 in **20** becomes longer than in **17**. Comparing the geometry and energy of the four highest transition states, **2**, **11**, **16**, and **19**, it is easy to see that the tight fragments of **2**, **11**, and **19** are all the same as **16**. The loosely bonded parts do not affect the activation energy more than 1 kcal/mol, although such an effect has been confirmed when SiH_4 interacts with a strong Lewis acid, such as B_2H_6.[31] Therefore, it can be concluded that the rate-limiting step along all four of the routes is the self-dissociation of SiH_4 into $SiH_2{-}H_2$. However, the formation of $SiH_2{-}H_2$ does not necessarily result in Si−Si bond formation. The nucleation requires another SiH_4 in close proximity as an attacker; otherwise, $SiH_2{-}H_2$ will go back to SiH_4 rather than to Si_2H_6.

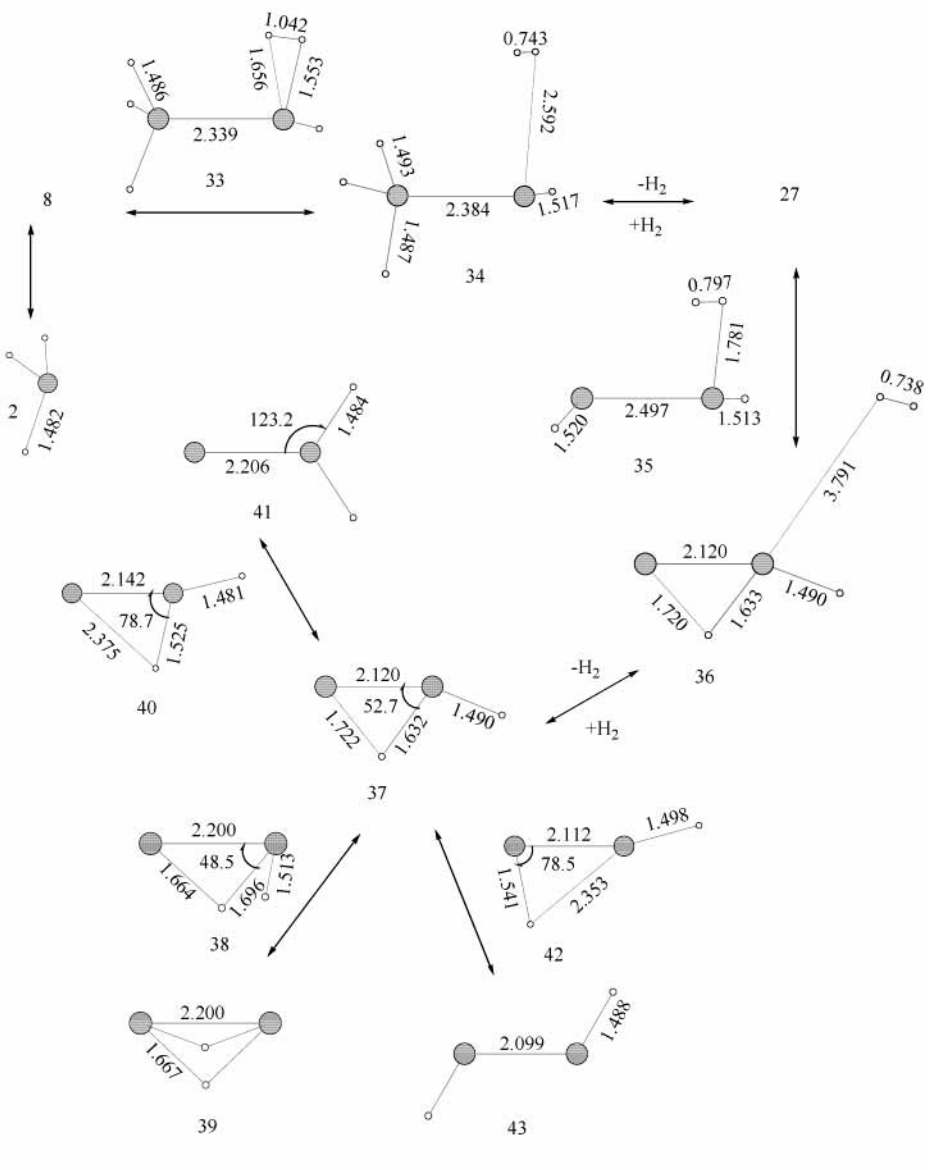

III

Figure 4. Optimized (MP2/6-31+G*) geometry structures of the species involved in third H_2 elimination of the reaction paths (III). Bond lengths are in Å, angles are in degree. The species on or under the double arrows are transition states.

Part (II): Second H_2 Elimination and the Formation of Five Si_2H_4 Isomers. In addition to the reversed reaction, Si_2H_6 can undergo further dissociations. Both compound **9** and its isomer **14** are complexes of SiH_4 and SiH_2 monomers bridged by a hydrogen bond. Compound **14** is 1.18 kcal/mol more stable than **9**, in agreement with previous calculations.[20,21] It is interesting to note that the mono-hydrogen-bridged bond in both species bears some resemblance to that appearing in complex SiH_4-BH_3,[32,33] indicating a similarity between SiH_2 and BH_3 fragments. Compound **9** is more reactive than **14** toward further H_2 elimination because its bridged hydrogen is structurally feasible to combine with a hydrogen atom from either the SiH_3 or the SiH_2 group. Compound **9** can, thus, eliminate the second H_2 in two ways. The first way requires 89.57 kcal/mol energy for the system to reach the transition state $H_2-SiH_2SiH_2$_t (**21**) and the H_2-eliminated product $H_2-SiH_2SiH_2$ (**22**) or SiH_2SiH_2 (**23**), which is the most stable one among five Si_2H_4 isomers. Compound **23** shows an unusual topological feature. Three critical points are located between the two Si atoms: two of them are (3, −1) bond critical points, whereas the one at the center is a (3, −3) critical point. Such a point is a maximum on the electron density surface and is usually associated with a nucleus. Different from its carbon analogue, C_2H_4, the four hydrogen atoms in **23** are not in the same plane. Compound **23** can isomerize into SiH_2HSiH (**25**) over a transition state SiH_2-SiH_2_t (**24**). The seemingly mono-hydrogen bridge in **25** is not formed according to the AIM calculation, perhaps because of the strain of the three-member ring. Compound **25** then goes to SiH_3SiH (**27**) over transition state SiH_2HSiH_t (**26**). It should be noted that **27** can be produced by self-H_2-elimination from **8** (part III) over a much lower energy barrier. The isomers **25** and **23** are, thus, more likely to be produced from **27**, rather than to overcome the high barrier transition state **21**. The second way of eliminating a H_2 from **9** requires 108.22 kcal/mol energy for the system to reach another transition state, SiH_2HSH_2H_t (**28**). The interesting structure of **28** contains a bridged hydrogen and a ring of three hydrogen atoms from which H_2 elimination takes place, resulting in $HSiH_2SiH-H_2$ (**29**) or $HSiH_2SiH$ (**30**), which is a diborane (B_2H_6)-like ring structure with a double hydrogen-bridged bond and two trans terminal hydrogen atoms. Compound **30** has a less stable isomer with cis terminal hydrogen atoms $HSiH_2SiH$_*cis* (**32**). The transition state of

TABLE 2: Electronic Energies, Dipole Moments, and Rotational Constants of the Species

no.	species	symm[a]	E_e [b] (a.u.)	ZPE[c] (kcal/mol)	dipole[b] (Debye)	rotational constants[c] GHZ		
	H_2	$D_{\infty h}(0)$	−1.16030	6.48	0.000	0.000	1842	1842
	SiH_4	$T_d(0)$	−291.49669	20.34	0.000	85.71	85.71	85.71
	$SiH_3{\cdot}$	$C_{3v}(0)$	−290.85273	13.91	0.168	141.8	141.8	83.72
	SiH_2	$C_{2v}(0)$	−290.23618	7.669	0.209	244.9	207.9	112.5
1	$SiH_4{-}SiH_4$	C_1 (0)	−582.99452	41.19	0.007	42.81	1.583	1.582
2	$SiH_4{-}SiH_2H_2$a_t	C_1 (1)	−582.89319	38.23	0.381	38.36	1.603	1.597
3	$SiH_4{-}SiH_2{-}H_2$	C_1 (0)	−582.89928	37.47	0.683	31.34	1.561	1.535
4	$SiH_4{-}SiH_2{-}H_2$_t	C_1 (1)	−582.89884	37.31	0.595	35.67	1.562	1.546
5	$SiH_3HSiH_2{-}H_2$ a	C_1 (0)	−582.90704	38.06	1.814	46.44	2.890	2.884
6	$SiH_3HSiH_2{-}H_2$a_ t	C_1 (1)	−582.90600	37.79	1.079	36.13	3.269	3.223
7	$SiH_3SiH_3{-}H_2$	C_1 (0)	−582.98300	38.58	0.010	10.05	4.981	3.609
8	SiH_3SiH_3	D_{3d} (0)	−581.82238	31.89	0.000	43.07	5.084	5.084
9	SiH_3HSiH_2a	C_s (0)	−581.74608	31.13	1.832	47.58	4.050	4.027
10	SiH_3HSiH_2a _t	C_s (1)	−581.74535	30.90	1.057	46.94	4.811	4.764
11	$SiH_4SiH_2{-}H_2$b_ t	C_1 (2)	−582.89317	38.25	0.261	45.19	1.637	1.632
12	$SiH_3HSiH_2{-}H_2$b	C_1 (0)	−582.90880	38.17	2.203	28.84	2.780	2.684
13	$SiH_3HSiH_2{-}H_2$b_t	C_1 (2)	−582.90924	37.77	1.282	20.91	3.328	3.066
14	SiH_3HSiH_2b	C_1 (0)	−581.74797	31.09	2.269	48.65	3.500	3.485
15	SiH_3HSiH_2b_t	C_s (1)	−581.74860	31.04	1.301	46.97	4.395	4.379
16	$SiH_2{-}H_2$_t	C_s (0)	−291.39492	17.40	0.326	103.4	81.00	69.12
17	$SiH_2{-}H_2$	C_s (0)	−291.40067	16.53	0.490	108.8	37.28	36.61
18	$SiH_4{-}H_2$	C_1 (0)	−292.65721	27.09	0.014	81.91	12.56	12.48
19	$H_2{-}SiH_2{-}H_2$_t	C_1 (1)	−292.55546	24.31	0.330	77.12	10.51	10.07
20	$H_2{-}SiH_2{-}H_2$	C_1 (0)	−292.56244	24.27	0.330	79.11	17.18	16.35
21	$H_2{-}SiH_2SiH_2$_t	C_s (1)	−581.68197	28.74	2.707	41.02	5.227	5.195
22	$H_2{-}SiH_2SiH_2$	C_1 (0)	−581.73544	27.10	0.007	35.70	3.979	3.921
23	SiH_2SiH_2	C_{2h} (0)	−580.57481	20.26	0.000	75.65	6.383	5.960
24	SiH_2SiH_2_t	C_1 (1)	−580.54060	18.72	2.187	70.69	6.204	5.993
25	SiH_2HSiH	C_1 (0)	−580.56323	20.37	1.281	73.54	6.233	5.975
26	SiH_3SiH_t	C_1 (1)	−580.55959	19.71	1.056	69.02	6.020	5.803
27	SiH_3SiH	C_s (0)	−580.56292	19.94	0.266	62.55	5.459	5.331
28	SiH_2HSiH_3H _t	C_s (2)	−581.64961	27.08	2.063	45.68	4.154	4.119
29	$HSiH_2SiH{-}H_2$	C_1 (0)	−581.70284	27.76	0.022	15.50	4.490	3.694
30	$HSiH_2SiH$	C_{2h} (0)	−580.54196	20.93	0.000	76.68	5.101	4.985
31	$HSiH_2SiH$ _t	C_1 (1)	−580.51708	19.64	0.660	73.15	5.003	4.878
32	$HSiH_2SiH$_*cis*	C_{2v} (0)	−580.53783	20.78	0.695	77.02	4.991	4.879
33	$SiH_3SiH{-}H_2$_t	C_1 (1)	−581.73081	29.42	0.481	40.90	5.240	5.120
34	$SiH_3SiH{-}H_2$	C_1 (0)	−581.72652	28.20	0.665	24.16	5.141	4.645
35	$SiHSiH{-}H_2$_t	C_1 (1)	−580.46730	18.49	0.964	48.34	5.174	5.006
36	$SiHSiH{-}H_2$	C_1 (0)	−580.51158	16.03	0.978	33.25	5.204	4.505
37	SiHSiH	C_s (0)	−579.35079	9.25	0.937	265.7	7.340	7.143
38	SiHSiH_t	C_1 (1)	−579.34095	8.95	1.096	133.4	7.137	7.069
39	SiH_2Si	C_{2v} (0)	−579.36867	10.52	0.530	161.8	7.340	7.253
40	$SiSiH_2$ _t	C_s (1)	−579.33862	8.50	0.899	215.2	7.121	6.893
41	$SiSiH_2$	C_{2v} (0)	−579.34316	9.54	0.066	162.5	6.722	6.455
42	HSiSiH_ t	C_s (1)	−579.32540	8.25	1.603	213.7	7.295	7.054
43	HSiSiH	C_{2h} (0)	−579.33843	10.36	0.000	186.9	7.278	7.005

[a] Symmetry of the species, the number of imaginary frequency are in parentheses. [b] MP2/6-311++G**// MP2/6-31+G* calculations. [c] MP2/6-31+G*// MP2/6-31+G* calculations.

interconversion between **30** and **32** is $HSiH_2SiH$_t (**31**), which is 14.32 kcal/mol higher in energy than the trans isomer **30**. In a way anaologous to B_2H_6's self-dissociation into two BH_3's, **30** or **32** can dissociate into two monomers, SiH_2, and raise the system's energy to 113.58 kcal/mol. The dissociation energy from **32** to two SiH_2's is 35.63 kcal/mol, also comparable to that of B_2H_6. Indeed, containing only six valence electrons, SiH_2 behaves in some ways quite like the electron-deficient Lewis acid BH_3. It can be seen that the ring structures **30** and **32** are less stable than the other isomers of Si_2H_4, and they are relatively difficult to form because of the high barrier of **28** and the energetically demanding process for two SiH_2 species to join together. However, once formed, they could be trapped within the same high barriers for a period of time. Experimental evidence for the existence of **30** was reported very recently.[7] Compared with Si_2H_6, it is clear that Si_2H_4 has a stronger tendency to form the Si−H−Si bond.

Part (III): Third H_2 Elimination and the Formation of Four Si_2H_2 Isomers. The dissociation of disilane **8** into two SiH_3 radicals requires 73.91 kcal/mol, which is the energy sum of two SiH_3 and one H_2 relative to **1**. No transition states are located in the process. The total system is more stable as two SiH_3 than as two SiH_2 (113.58 kcal/mol) fragments. Alternatively, **8** can be regarded as a SiH_3 derivative of SiH_4. Its self-

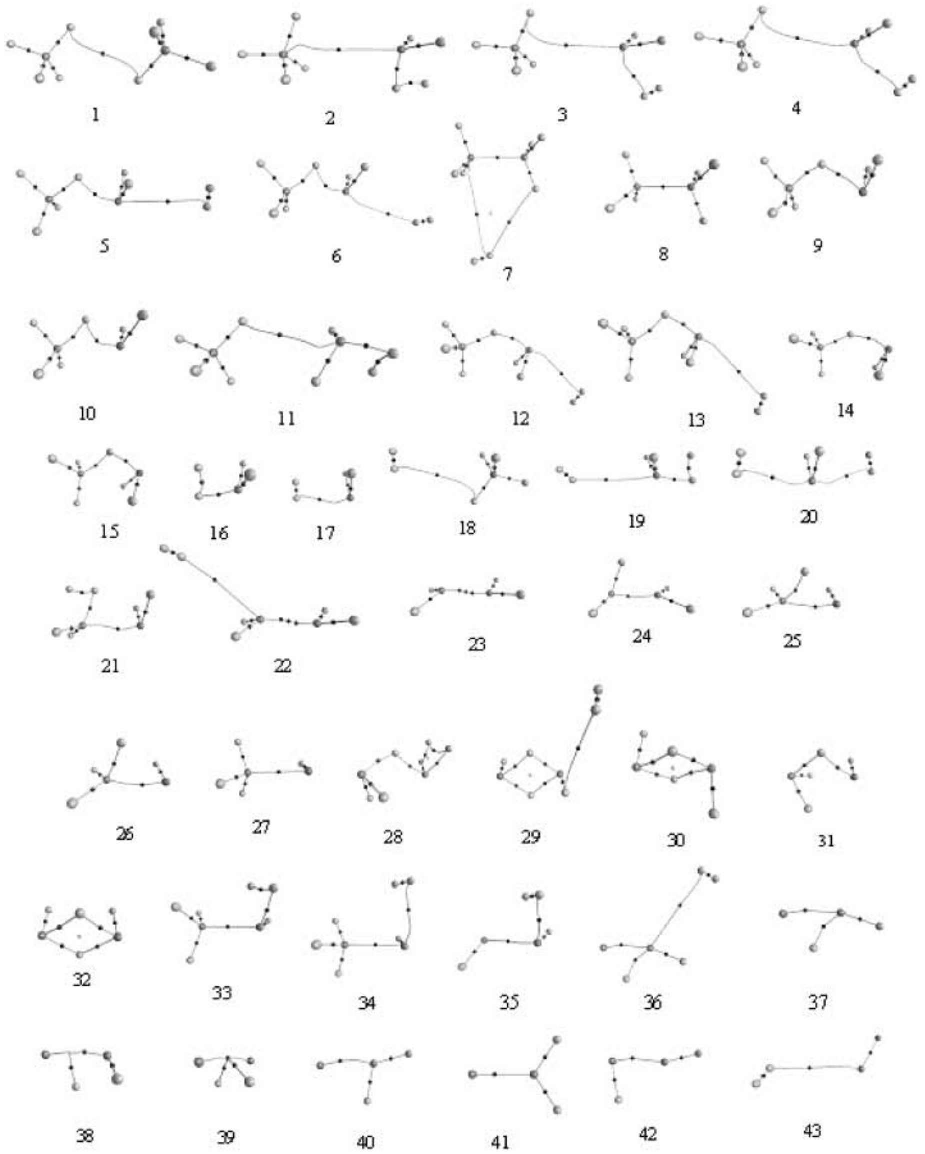

Figure 5. AIM (MP2/6-31+G*) calculated molecular graphs with bond paths and BCP for the species. The numbering order is same as in Table 1 and Figure 1.

dissociation, as an analogue of SiH_4 dissociating into SiH_2 and H_2, can be accomplished via two paths. One is the elimination of a SiH_4, an inverse of the silane nucleation; the other is the elimination of the second H_2. Of course, the H_2 elimination from Si_2H_6 can result in the larger nucleation product Si_3H_8 in a similar way as SiH_4 to Si_2H_6, described in Part I. In a two-silicon system, our present focus, the H_2 elimination from **8** produces a Si_2H_4 isomer $SiH_3SiH{-}H_2$ (**34**) or SiH_3SiH (**27**). Compound **27** is also a product in Part II and can be regarded as a SiH_3 derivative of the transient species SiH_2. The activation energy of the transition state $SiH_3SiH{-}H_2$_t (**33**) from **8** is 54.99 kcal/mol (59.60−4.61), which is ~1 kcal/mol lower than that required for H_2 elimination from SiH_4. The hydrogen content in **27** can still decrease by eliminating the third H_2 to form the Si_2H_2 species. The transition state $SiHSiH{-}H_2$_t (**35**) of the H_2 elimination requires 119.92 kcal/mol energy for the total system. The direct product of H_2 elimination from **27** is $SiHSiH{-}H_2$ (**36**) or SiHSiH (**37**). Geometrically, the two silicon atoms and a bridged hydrogen atom in **37** compose a three-member ring structure and possess plane symmetry, whereas the AIM calculation shows that the Si−H−Si bond is not formed, probably because of too much strain on a three member ring, the same reason that accounts for **25**. The most stable structure among the four isomers of Si_2H_2 is SiH_2Si (**39**), with double hydrogen-bridged bonds and a nonplane structure. The AIM calculation shows the unusual bonding nature of **39**. The bridged hydrogen atoms connect to the center of the Si−Si bond by the bond paths rather than the two silicon atoms. Unlike Si_2H_4, the two isomers $SiSiH_2$ (**41**) and HSiSiH (**43**) without the Si−H−Si bond are less stable than the bridged ones. Compound **41** with a bare silicon atom and C_{2v} symmetry is slightly more stable than **43** with C_{2h} symmetry. Compounds **41** and **43** can isomerize to the intermediate **37** through transition states $SiSiH_2$ _t (**40**) and HSiSiH_ t (**42**), respectively. Compound **37** then isomerizes to the most stable isomer **39** through transition state SiHSiH_t (**38**). Compared with Si_2H_4, Si_2H_2 has a stronger tendency to form the Si−H−Si bond.

IV. Concluding Remarks

The rate-limiting step of the first H_2 elimination is self-dissociation of SiH_4 to $SiH_2{-}H_2$. Sufficiently high pressure and concentration of SiH_4 are necessary to promote full H_2 elimination through the formation of two transient intermediates with

TABLE 3: Relative Energies of the Intermediate Species of the Si_2H_8 System

species[a]	D_e[c]	D_e[d]	D_{e0}[e]	species[a]	D_e[c]	D_e[d]	D_{e0}[e]
$2SiH_4$	0.58	0.72	0.21	$28 + 2H_2$	122.63	115.84	108.22
1	0.00	0.00	0.00	$29 + 2H_2$	82.91	82.44	75.50
2	66.95	63.58	60.62	$30 + 2H_2$	83.08	82.80	75.51
3	58.63	59.77	56.04	$31 + 2H_2$	98.24	98.42	89.83
4	58.67	60.04	56.16	$32 + 2H_2$	85.35	85.40	77.95
5	55.04	54.90	51.77	$2SiH_2 + 2H_2$	120.72	126.48	113.58
6	55.25	55.55	52.15	$8 + H_2$	3.66	7.43	4.61
7	3.52	7.23	4.62	$33 + H_2$	65.21	64.89	59.60
11	67.10	63.60	60.66	$34 + H_2$	62.06	67.58	61.07
12	53.86	53.79	50.76	$35 + 2H_2$	126.98	129.66	119.92
13	54.84	53.52	50.09	$36 + 2H_2$	94.48	101.87	89.67
$9 + H_2$	55.27	55.31	51.73	$37 + 3H_2$	94.66	102.18	89.68
$21 + H_2$	96.60	95.54	89.57	$38 + 3H_2$	100.90	108.35	95.56
$22 + H_2$	54.52	61.99	54.37	$39 + 3H_2$	86.60	90.96	79.73
$23 + 2H_2$	54.67	62.20	54.22	$40 + 3H_2$	99.59	109.81	96.56
$24 + 2H_2$	78.74	83.66	74.15	$41 + 3H_2$	95.63	106.96	94.76
$25 + 2H_2$	65.09	69.46	61.59	$42 + 3H_2$	108.30	118.11	104.61
$26 + 2H_2$	65.96	71.74	63.22	$43 + 3H_2$	99.01	109.93	98.54
$27 + 2H_2$	62.93	69.66	61.36	$2SiH_3\cdot + H_2$	76.83	80.80	73.91

species[b]	D_d[e]	D_e[e]	D_{e0}[f]	species[c]	D_e[d]	D_e[e]	D_{e0}[f]
SiH_4	0.00	0.00	0.00	18	0.00	0.00	0.00
16	67.27	63.86	60.92	19	67.26	63.85	61.07
17	58.98	60.25	56.44	20	58.28	59.47	56.64
$SiH_2 + H_2$	60.07	62.88	56.69				

[a] Species with electronic energies relative to Si_2H_8 (1). [b] Species with electronic energies relative to SiH_4. [c] Species with electronic energies relative to SiH_4-H_2 (16). [d] Relative electronic energies D_e (kcal/mol) calculated at the MP2/6-31+G*//MP2/6-31+G* level. See Table 1 for the species and Figure 1 for the structures. [e] Relative electronic energies, D_e (kcal/mol), calculated at the MP2/6-311++G**//MP2/6-31+G* level. [f] Relative electronic energies D_e (kcal/mol) calculated at the MP2/6-311++G**//MP2/6-31+G*+ ZPE level. These values are used in the discussion.

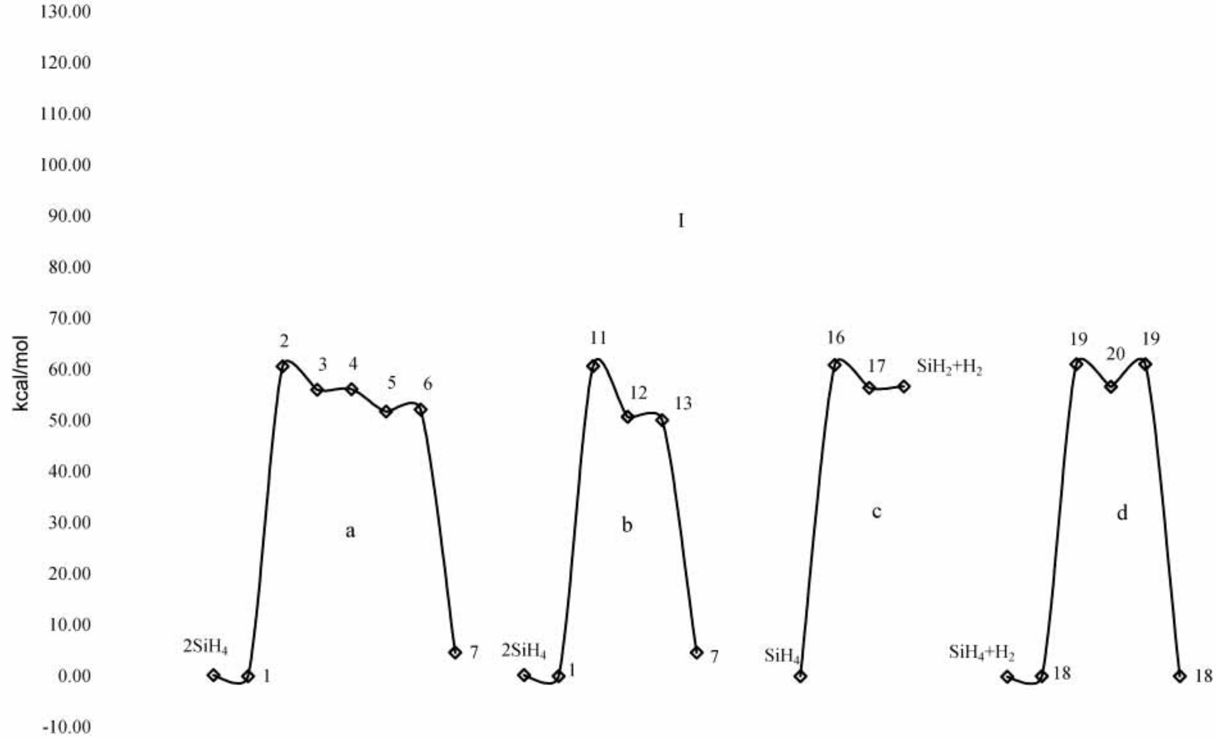

Figure 6. The initial reaction pathways started from SiH_4+SiH_4 (a), (b), one SiH_4 (c), and $SiH_4 + H_2$ (d) systems based on calculations at the MP2/6-311++G**//MP2/6-31+G*+ZPE level. See Table 2 for composition, Table 3 for relative energies, and Figure 1 for geometry structures of the species 1−20.

a Si−H−Si bond, which isomerize readily to the usual disilane. Eliminating a second H_2 from Si_2H_6 results in unsaturated silicon hydrides Si_2H_4. Among the five isomers of Si_2H_4, the ones without the Si−H−Si bond are more stable than those that do possess such a bond. Eliminating the third H_2 from one of the Si_2H_4 isomers results in silicon hydrides Si_2H_2. Among the four

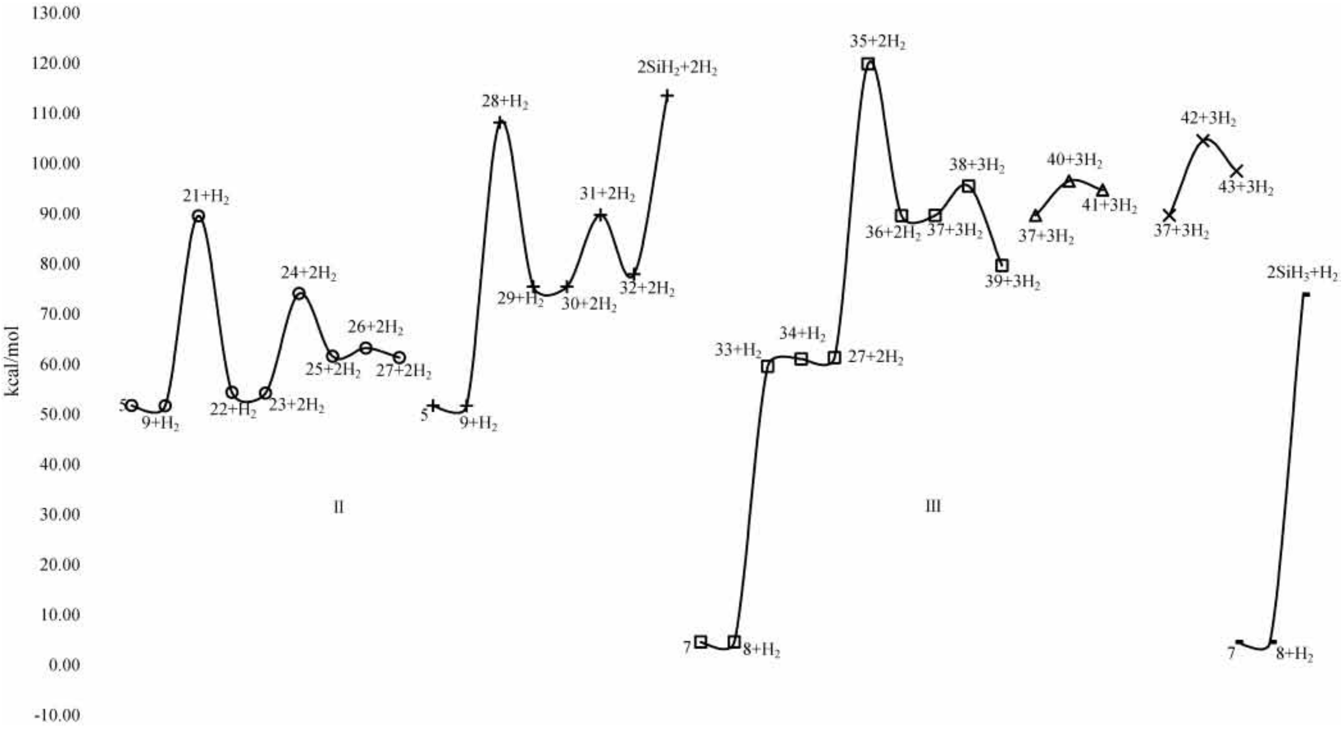

Figure 7. The reaction pathways for formation and isomerization of five Si_2H_4 (II), four Si_2H_4 isomers, and SiH_3 radicals (III) based on calculations at the MP2/6-311++G**//MP2/6-31+G*+ZPE level. See Table 2 for composition, Table 3 for relative energies, and Figure 1 for geometry structures of the species 21−43.

TABLE 4: Calculated Vibrational Frequency and IR Intensity of the Minimum Species[a]

	SiH_2	1066 (115), 2149 (304), 2150 (339)
	$SiH_3\cdot$	807 (105), 973 (80), 2302 (16), 2338 (153)
	SiH_4	959 (180), 2339 (160)
1	SiH_4- SiH_4	949 (421), 964 (317), 964 (323), 966 (17), 2332 (343), 2336 (26), 2337 (17), 2338 (280), 2340 (268)
3	$SiH_4-SiH_2-H_2$	108 (12), 611 (15), 952 (267), 960 (159), 961 (163), 1061 (83), 2156 (301), 2160 (303), 2319 (83), 2328 (142), 2337 (127), 2342 (139), 4372 (5)
5	$SiH_3HSiH_2-H_2$ a	484 (26), 677 (57), 1015 (74), 887 (49), 915 (575), 948 (114), 999 (72), 1015 (74), 1236 (357), 2017 (331), 2163 (215), 2173 (266), 2318 (135), 2369 (46), 2390 (85), 4513 (2)
7	$SiH_3SiH_3-H_2$	383 (32), 384 (32), 888 (594), 988 (107), 2294 (153), 2316 (270), 2316 (270), 2316 (266)
8	SiH_3SiH_3	383 (32), 888 (601), 988 (106), 2295 (155), 2316 (267)
9	SiH_3HSiH_2a	497 (19), 672 (39), 875 (43), 915 (550), 945 (145), 1002 (75), 1014 (73), 1282 (380), 1974 (291), 2165 (215), 2176 (259), 2314 (139), 2368 (44), 2390 (84)
12	$SiH_3HSiH_2-H_2$b	450 (36), 657 (14), 701 (118), 925 (373), 952 (95), 982 (90), 987 (19), 1025 (77), 1237 (94), 1929 (502), 2121 (248), 2144 (261), 2345 (89), 2371 (87), 2394 (77)
14	SiH_3HSiH_2b	459 (29), 657 (14), 698 (108), 924 (374), 951 (95), 983 (94), 986 (21), 1025 (81), 1260 (89), 1909 (489), 2119 (250), 2143 (265), 2143 (265), 2345 (91), 2372 (86), 2395 (77)
17	SiH_2-H_2	117 (10), 588 (13), 1056 (98), 2155 (272), 2159 (336), 4389 (6)
18	SiH_4-H_2	960 (182), 960 (177), 960 (180), 2336 (162), 2337 (155), 2337 (159)
20	$H_2-SiH_2-H_2$	565 (16), 1053 (89), 2157 (257), 2161 (336), 4446 (8), 4448 (2)
22	$H_2-SiH_2SiH_2$	349 (21), 471 (19), 938 (196), 2318 (131), 2352 (183)
23	SiH_2SiH_2	348 (21), 469 (20), 939 (195), 2316 (131), 2350 (185)
25	SiH_2HSiH	424 (10), 468 (23), 500 (21), 668 (8), 736 (35), 906 (115), 994 (74), 1055 (388), 1733 (132), 2137 (203), 2300 (157), 2324 (139)
27	SiH_3SiH	398 (13), 410 (40), 453 (32), 750 (70), 910 (252), 959 (89), 983 (42), 2137 (229), 2268 (104), 2280 (139), 2305 (151)
29	$HSiH_2SiH-H_2$	309 (3), 739 (18), 877 (205), 1386 (49), 1571 (1283), 2170 (458)
30	$HSiH_2SiH$	308 (3), 738 (16), 878 (206), 1385 (48), 1571 (1282), 2170 (464)
32	$HSiH_2SiH$_*cis*	402 (2), 790 (118), 911 (23), 958 (58), 1366 (55), 1496 (1659), 2165 (17), 2190 (430)
34	SiH_3SiH-H_2	353 (19), 380 (6), 443 (35), 465 (18), 474 (66), 2143 (225), 2260 (111), 2290 (134), 2302 (149)
36	$SiHSiH-H_2$	208 (40), 475 (6), 616 (18), 1192 (246), 1729 (84), 2264 (123), 4521 (1)
37	SiHSiH	204 (41), 470 (6), 615 (18), 1189 (247), 1730 (83), 2263 (124)
39	SiH_2Si	1004 (52), 1266 (466), 1622 (10), 1716 (5)
41	$SiSiH_2$	271 (37), 343 (9), 537 (18), 920 (70), 2287 (67), 2318 (90)
43	HSiSiH	498 (35), 964 (806), 2276 (161)

[a] Frequencies are in cm^{-1}. Intensities (in parentheses) are in km/mol. MP2/6-31+G* calculation.

isomers of Si_2H_2, the isomer with a double Si−H−Si bond is the most stable one. To initiate the gas-phase reactions, ~60−61 kcal/mol is required to reach the activation energy of the first H_2 elimination and subsequent nucleation. To obtain species with two silicon and fewer hydrogen atoms generally requires more energy for the system. Within the energy range of 120 kcal/mol, breaking the Si−Si bond to form two SiH_2 or two SiH_3 radical species are also possible processes.

References and Notes

(1) Pauleau, Y.; Tonneau, D. *J. Appl. Phys.* **2002**, *91*, 1553.

(2) Pola, J.; Santos, M.; Diaz, L.; Jursikova, K. N.; Bastl, Z.; Bohacek, J.; Fajgar, R.; Urbanova, M. *J. Mater. Chem.* **2002**, *12*, 1519.

(3) Amanatides, E.; Stamou, S.; Mataras, D. *J. Appl. Phys.* **2001**, *90*, 5786.

(4) Kim, K. C.; Reed, C. A.; Elliott, D. W.; Mueller, L. J.; Tham, F.; Lin, L. J.; Lambert, J. B. *Science* **2002**, *297*, 825.

(5) Girshick, S. L. *J. Chem. Phys.* **1997**, *107*, 1948.

(6) Sriraman, S.; Agarwal, S.; Aydil, E. S.; Maroudas, D. *Nature* **2002**, *418*, 62.

(7) Andrews, L.; Wang, X. F. *J. Phys. Chem. A* **2002**, *106*, 7696.

(8) Chambreau, S. D.; Wang, L. M.; Zhang, J. S. *J. Phys. Chem. A* **2002**, *106*, 5081.

(9) Rechtsteiner, G. A.; Hampe, O.; Jarrold, M. F. *J. Phys. Chem. B* **2001**, *105*, 4188.

(10) Chambreau, S. D.; Zhang, J. S. *Chem. Phys. Lett.* **2001**, *343*, 482.

(11) Wehrspohn, R. B.; Deane, S. C.; French, I. D.; Gale, I.; Hewett, J.; Powell, M. J.; Robertson, J. *J. Appl. Phys.* **2000**, *87*, 144.

(12) Zellama, K.; Nedialkova, L.; Bounouh, Y.; Chahed, L.; Benlahsen, M.; Zeinert, A.; Paret, V.; Theye, M. L. *J. Non-Cryst. Solids* **1996**, *200*, 81.

(13) Kessels, W. M. M.; Severens, R. J.; Smets, A. H. M.; Korevaar, B. A.; Adriaenssens, G.. J.; Schram, D. C.; van de Sanden, M. C. M. *J. Appl. Phys.* **2001**, *89*, 2404.

(14) Suda, Y.; Hosoya, N.; Shiratori, D. *J. Cryst. Growth* **2002**, *237*, 1404.

(15) Markus, M. W.; Roth, P. A. *J. Quant. Spectrosc. RA* **1994**, *52*, 783.

(16) Heintze, M.; Bauer, G. H. *J. Phys. D Appl. Phys.* **1995**, *28*, 2470.

(17) Jasinski, J. M.; Becerra, R.; Walsh, R. *Chem. Rev.* **1995**, *95*, 1203.

(18) Tonokura, K.; Murasaki, T.; Koshi, M. *J. Phys. Chem. B* **2002**, *106*, 555.

(19) Becerra, R.; Frey, H. M.; Mason, B. P.; Walsh, R.; Gordon, M. S. *J. Am. Chem. Soc.* **1992**, *114*, 2751.

(20) Becerra, R.; Frey, H. M.; Mason, B. P.; Walsh, R.; Gordon, M. S. *J. Chem. Soc., Faraday Trans.* **1995**, *91*, 2723.

(21) Swihart, M. T.; Carr, R. W. *J. Phys. Chem. A* **1997**, *101*, 7434.

(22) Walch, S. P.; Dateo, C. E. *J. Phys. Chem. A* **2001**, *105*, 2015.

(23) Kang, J. K.; Musgrave, C. B. *Phys. Rev. B* **2001**, *64*, 245330.

(24) Swihart, M. T.; Girshick, S. L. *J. Phys. Chem. B* **1999**, *103*, 64.

(25) Katzer, G.; Ernst, M. C.; Sax, A. F.; Kalcher, J. *J. Phys. Chem. A* **1997**, *101*, 3942.

(26) Peng, C. Y.; Ayala, P. Y.; Schlegel, H. B.; Frisch, M. J. *J. Comput. Chem.* **1996**, *17*, 49.

(27) Frisch, M. J.; Trucks, G. W.; Schlegel, H. B.; Scuseria, G. E.; Robb, M. A.; Cheeseman, J. R.; Zakrzewski, V. G.; Montgomery, J. A., Jr.; Stratmann, R. E.; Burant, J. C.; Dapprich, S.; Millam, J. M.; Daniels, A. D.; Kudin, K. N.; Strain, M. C.; Farkas, O.; Tomasi, J.; Barone, V.; Cossi, M.; Cammi, R.; Mennucci, B.; Pomelli, C.; Adamo, C.; Clifford, S.; Ochterski, J.; Petersson, G. A.; Ayala, P. Y.; Cui, Q.; Morokuma, K.; Malick, D. K.; Rabuck, A. D.; Raghavachari, K.; Foresman, J. B.; Cioslowski, J.; Ortiz, J. V.; Stefanov, B. B.; Liu, G.; Liashenko, A.; Piskorz, P.; Komaromi, I.; Gomperts, R.; Martin, R. L.; Fox, D. J.; Keith, T.; Al-Laham, M. A.; Peng, C. Y.; Nanayakkara, A.; Gonzalez, C.; Challacombe, M.; Gill, P. M. W.; Johnson, B. G.; Chen, W.; Wong, M. W.; Andres, J. L.; Head-Gordon, M.; Replogle, E. S.; Pople, J. A. *Gaussian 9*8, revision A.7; Gaussian, Inc.: Pittsburgh, PA, 1998.

(28) Biegler-Konig, F.; Schonbohm, J.; Bayles, D. *J. Comput. Chem.* **2001**, *22*, 545.

(29) Bader, R. F. W. *Atoms in Molecules: A Quantum Theory*; Oxford University Press: Oxford, U.K., 1990.

(30) Tsuzuki, S.; Uchimaru, T.; Mikami, M.; Urata, S. *J. Chem. Phys.* **2002**, *116*, 3309.

(31) Hu, S. W.; Wang, X. Y. *J. Phys. Chem. A* **2003**, *107*, 1635.

(32) Hu, S. W.; Kim, J.; Tarakeshwar, P.; Kim, K. S. *J. Phys. Chem. A* **2002**, *106*, 6817.

(33) Hu, S. W.; Wang, X. Y. *J. Phys. Chem. A* **2002**, *106*, 9558.